*Tellus* (1990), *42A*, 165–173

# A study of non-forecasted cyclogenesis in a polar air mass over the Baltic Sea

By KAI MYRBERG[1], JARMO KOISTINEN[1] and SIMO JÄRVENOJA[2], [1]*Department of Meteorology, University of Helsinki, Hallituskatu 11-13, SF-00100, Helsinki, Finland,* [2]*Finnish Meteorological Institute, Box 503, SF-00101, Helsinki, Finland*

(Manuscript received 2 November 1988; in final form 8 May 1989)

ABSTRACT

We present a case study of a developing meso-scale low in a cold air mass where baroclinicity was weak. Both mid-tropospheric vorticity advection and enhanced organized convection over the Baltic Sea seem to have caused the initial development. Later, baroclinic instability took over the dominating role in the development. The low studied exhibited properties of both polar lows and comma clouds. The case was simulated by a high-resolution limited area numerical model, which failed to develop the intense meso-scale part of the surface cyclone, probably because of too coarse a resolution.

## 1. Introduction

Traditionally, polar air vortices are divided into "polar lows" and "comma clouds" (Reed, 1979; Rasmussen, 1981; Locatelli et al., 1982; Reed and Blier, 1986; Businger, 1985, 1987). A comma cloud develops close to a trailing polar front, and strong baroclinicity is present through a deep tropospheric layer. A polar low develops further into the polar air. Usually, polar lows are meso-scale phenomena with a diameter of 100–500 km, whereas comma clouds have a larger extent (diameter 500–1500 km).

The mechanisms behind the formation and the development of polar lows are not fully understood. Baroclinic instability has been proposed as a possible mechanism (see e.g., Harrold and Browning, 1969; Mansfield, 1974; Reed, 1979; Uccellini, 1986; Orlanski, 1986). Another possibility is the CISK (Conditional Instability of the Second Kind) mechanism (see e.g., Rasmussen, 1977, 1979, 1985; Bratseth, 1985; Økland and Schyberg, 1987; Økland, 1987). It has also been suggested that both baroclinic instability and CISK are needed to initiate the development of polar lows (see e.g., Sardie and Warner, 1983, 1985; Forbes and Lottes, 1985; Craig and Cho, 1988).

In this paper, we present a case study of a rapidly developing meso-scale low, which formed over the Baltic Sea (58° N, 18° E) in a cold air mass on 23 October 1986. The synoptic situation and the development of the low is described in Section 2. In Section 3, simulations with a high resolution numerical model are described. Instability mechanisms responsible for the formation of the low studied are discussed in Section 4.

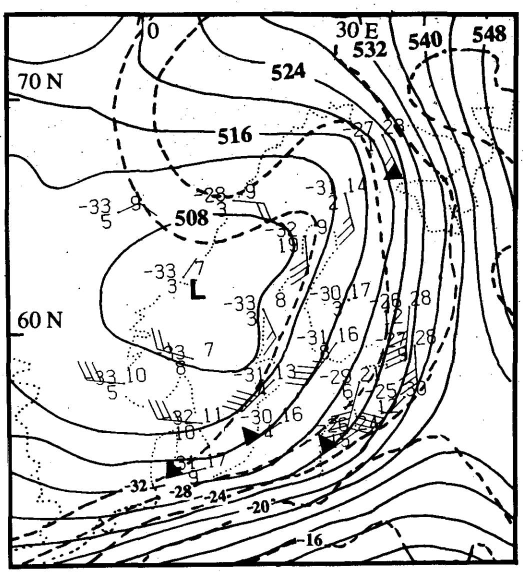


*Fig. 1.* The 500 mb geopotential height for 00 GMT, 23 October 1986 (solid lines: geopotential height in dam, dashed lines: temperature in °C).

## 2. Synoptic description of the low

During the cyclone development over the Baltic Sea, the large-scale synoptic situation in northern Europe was characterized by a cold low (Fig. 1). The upper-level low was moving eastwards, later northeastwards. The upper-level jet maximum was situated south of the Baltic Sea; a cold air mass was present over Scandinavia throughout the episode.

Satellite images show that the surface low development was coupled with the expanding cumulonimbus cloud clusters over the Baltic Sea (Fig. 2). This meso-scale cloud pattern (diameter approx. 300 km), denoted as B, as also cloud pattern A preceding it, actually existed about 24 h earlier over the North Sea as one of the cumulonimbus cloud systems formed in the cold air mass. Cloud pattern B moved across the southern part of Scandinavia and reached the Baltic Sea at about 22 GMT on 22 October, when the formation of the surface low started. At the beginning of the surface low development, there was a small-scale trough north of the island of Gotland (57° N, 18° E) with a minimum pressure of 977 mb (Fig. 3). Both ahead of and behind the trough there were three-hourly pressure falls of 1–3 mb. Thunderstorms, showers and continuous rain were observed in this area. The sea surface temperature varied between +7°C and +9°C and the temperature of the air, which advected over the sea, was from 2°C to 5°C. The wind speed over the Baltic Sea was from 5 m $s^{-1}$ to 12 m $s^{-1}$. The sensible heat flux, calculated by simple bulk-aerodynamic formulae, varied between 50 W $m^{-2}$ and 200 W $m^{-2}$, while the latent heat flux was about 100 W $m^{-2}$.


*Fig. 2.* NOAA IR satellite image at 0326 GMT, 23 October 1986. A and B denote cloud systems related to the cyclogenesis (see text). Surface fronts are shown.

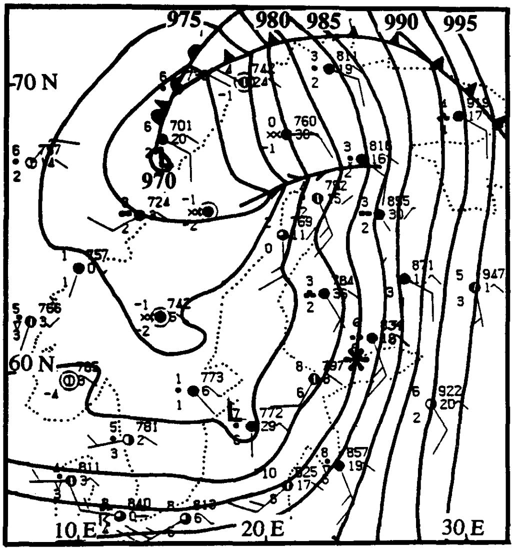


*Fig. 3.* Surface analysis together with some observations for 00 GMT, 23 October 1986. Solid lines denote pressure based on all observations. An asterisk denotes the location of the radar in Helsinki.

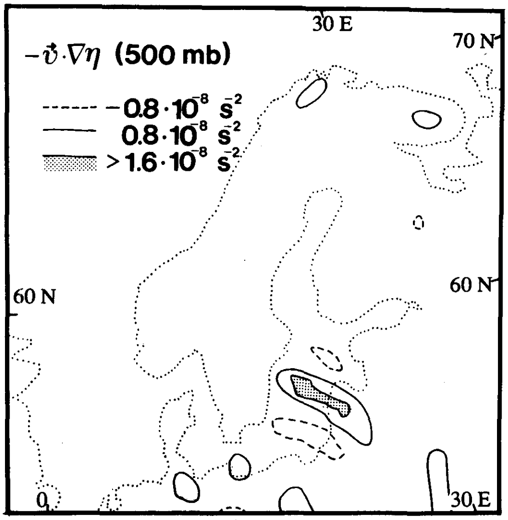


*Fig. 4.* Absolute vorticity advection at the 500 mb level 00 GMT, 23 October 1986. Isoline spacing shown in the figure.

The area of cyclogenesis was located about 700 km north of the surface polar front (Fig. 2). The sounding from Visby (57°N, 18°E) at 00 GMT 23 October (not shown) indicates that the air mass was cold and weakly baroclinic. The temperature advection was weak and the stratification was moist adiabatic from the surface up to the 430 mb level. Ahead of the synoptic-scale upper-level trough the 500 mb relative vorticity had a value of $1 \times 10^{-4}$ $s^{-1}$ and was associated with strong 500 mb vorticity advection (maximum value $2 \times 10^{-8}$ $s^{-2}$; Fig. 4).

During the next 12 h, the surface trough intensified and moved northeastwards. Simultaneously with the intensification of the surface trough, cloud pattern B and its related cumulonimbus clusters merged and became comma-shaped, and the area of the cloud system rapidly enlarged (Figs. 2, 5). Despite quite strong pressure falls (−3 mb/3 h), there was no surface low development in connection with pattern A (Fig. 3).

At 09 GMT, the low was located in southern Finland. In the southern part of the low, the pressure gradient was very strong. In radar measurements (at Helsinki, 60° N, 25°E), the vortex can be seen as a spiral-shaped precipitation pattern at the tip of the comma cloud (Fig. 6). In Fig. 6a, at 0908 GMT, the spiral-shaped rain-bands west of the radar are located below the head of the comma cloud (see Fig. 5). The fine structure of the vortex in Fig. 6b shows, at 1014 GMT, another well-developed precipitation spiral northeast of the radar. This pattern, whose diameter was about 30 km, was located in the area of the surface meso-scale low or trough. According to three-dimensional radar measurements, the height of the precipitating cloud was 7 km. In southern Finland, the total amount of rainfall (10–20 mm) was not especially large during the passage of the system.

At 12 GMT, the pressure gradient was at its most intense, and the low was located over southern and central Finland with a minimum pressure of 972 mb (Fig. 7). Ahead of the low there were pressure falls of 2–4 mb/3 h; behind it, the pressure rise was at most 7 mb/3 h concen-

tendencies and high wind speeds. The comma-

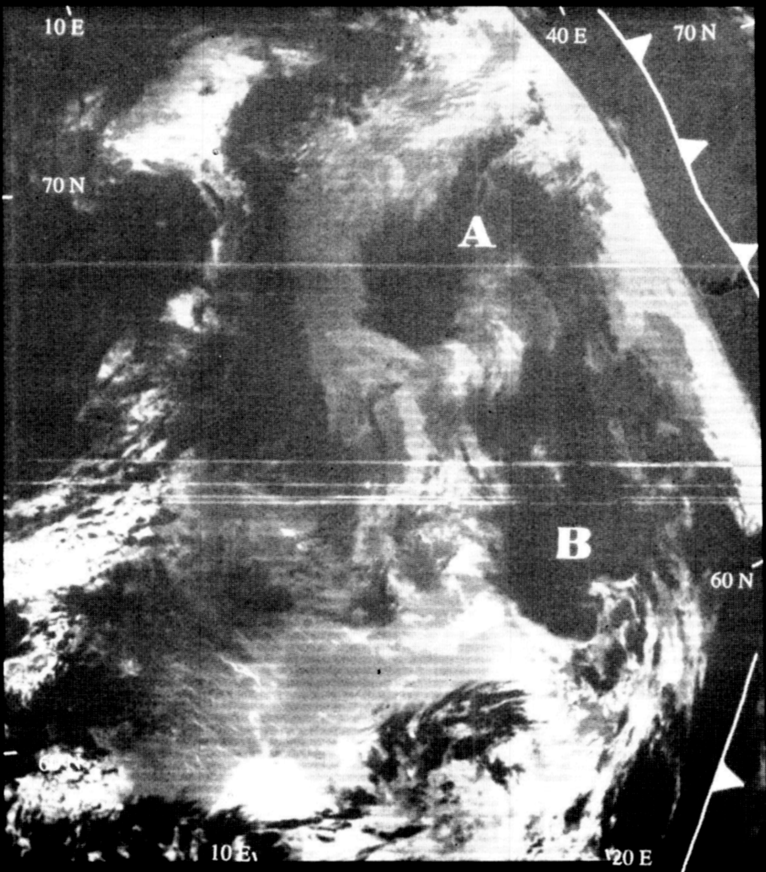


*Fig. 5.* NOAA IR satellite image at 0736 GMT, 23 October 1986. Notation as in Fig. 2.

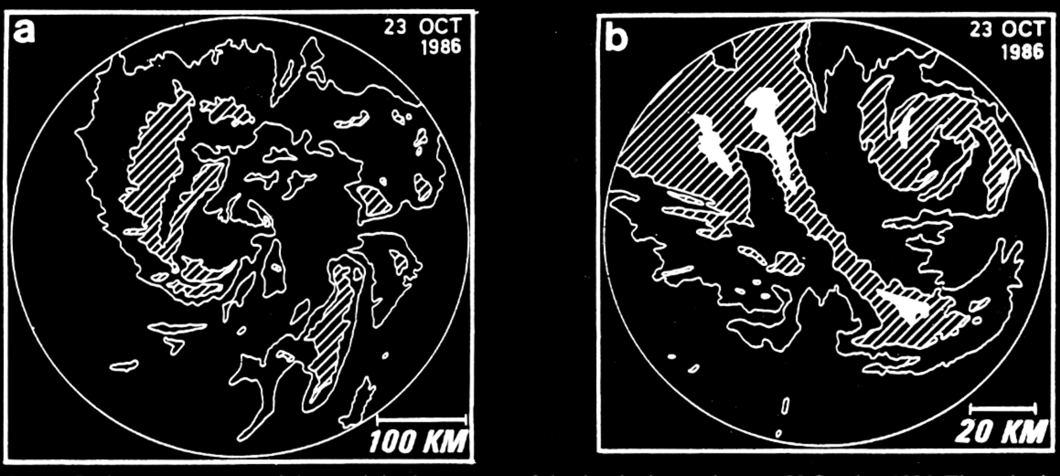


*Fig. 6.* Radar measurement of the precipitation pattern of the developing cyclone on 23 October 1986. The radar is located in the centre of the circle in Helsinki (see Fig. 3). The solid line denotes the boundary of slight rainfall, hatching denotes moderate rainfall (reflectivity factor 10 $dBZ_e$–30 $dBZ_e$) and black areas are heavy rainfall (> 30 $dBZ_e$). (a) 0908 GMT, measurement radius 256 km. (b) 1014 GMT, measurement radius 64 km.

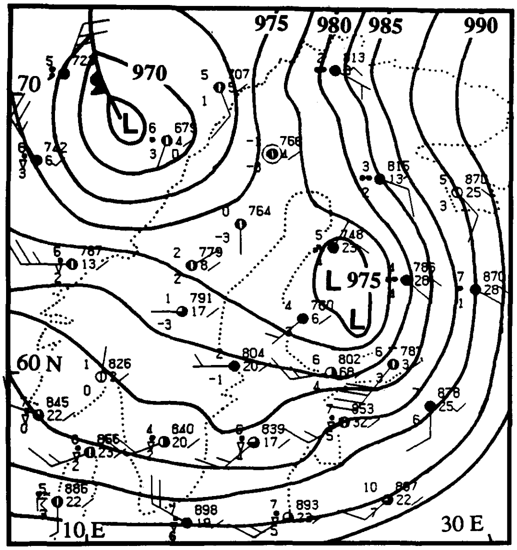


*Fig. 7.* Surface analysis for 12 GMT, 23 October 1986. Notation as in Fig. 3.

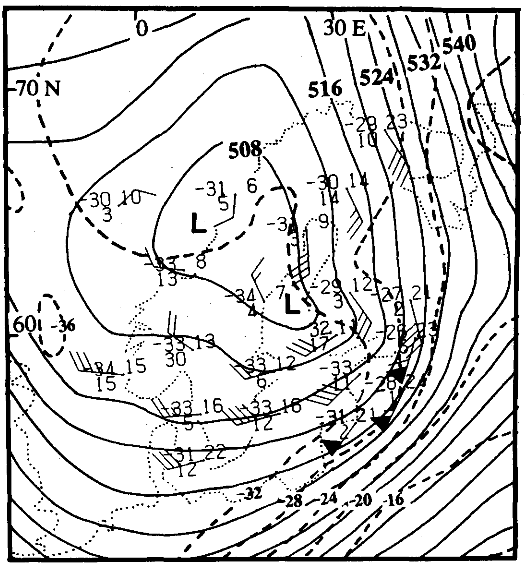


*Fig. 8.* The 500 mb analysis for 12 GMT, 23 October 1986. Notation as in Fig. 1.

shaped cloud pattern B (or the combined patterns A and B) formed a so-called instant occlusion (Browning and Hill, 1985) together with the cloud band of the polar front.

According to the vertical cross-section (not shown), the low was located in a cold weakly-baroclinic air mass lacking any strong evidence of frontal structure. In the sounding from Jokioinen (southern Finland) at 12 GMT 23 October (not shown), the stratification of the atmosphere was conditionally unstable up to 350 mb. The height of the tropopause was about 350 mb, which is quite typical for a polar low (see e.g., Lystad, 1986). The 500 mb analysis for 12 GMT 23 October (Fig. 8) shows that during the previous 12 h, the shape of the upper-level trough over the Baltic Sea had sharpened considerably. The 500 mb relative vorticity had a value of $1 \times 10^{-4}\ \mathrm{s}^{-1}$, while the vorticity advection had weakened to $1 \times 10^{-8}\ \mathrm{s}^{-2}$. The 850 mb relative vorticity had increased in 12 h from $5 \times 10^{-5}\ \mathrm{s}^{-1}$ to $1 \times 10^{-4}\ \mathrm{s}^{-1}$. Hence the strongest cyclonic development took place near the surface.

After its most intense stage at 12 GMT, the low moved northwards. It deepened about 2 mb in 12 h, but the surface pressure gradients decreased considerably. The cloud pattern of the low was spiral-shaped with a scale of about 1000 km. It had a visual resemblance to a classical occluded cyclone. However, there was no clear evidence of frontal structure. The low continued towards the Arctic Sea, remaining visible on weather maps for several days. The whole development of the cloud pattern from the comma stage to a mature cyclone is very similar to that in the conceptual model of Zick (1983).

## 3. Numerical simulations

The case studied has been simulated by the HIRLAM (High Resolution Limited Area Modelling) model, which was developed by a joint Nordic–Dutch project on limited area modelling during 1985–88. The HIRLAM data assimilation system consists of an analysis scheme, an initialization scheme and a forecast model. The analysis scheme is that of ECMWF (European Centre for Medium Range Weather Forecasts; see Lönnberg and Shaw, 1987), modified for a limited area by the HIRLAM group (see Gustafsson and Järvenoja, 1987). The initialization method used is a non-linear normal mode scheme for a limited area (Bijlsma and Hafkenscheid, 1984). The forecast model used is

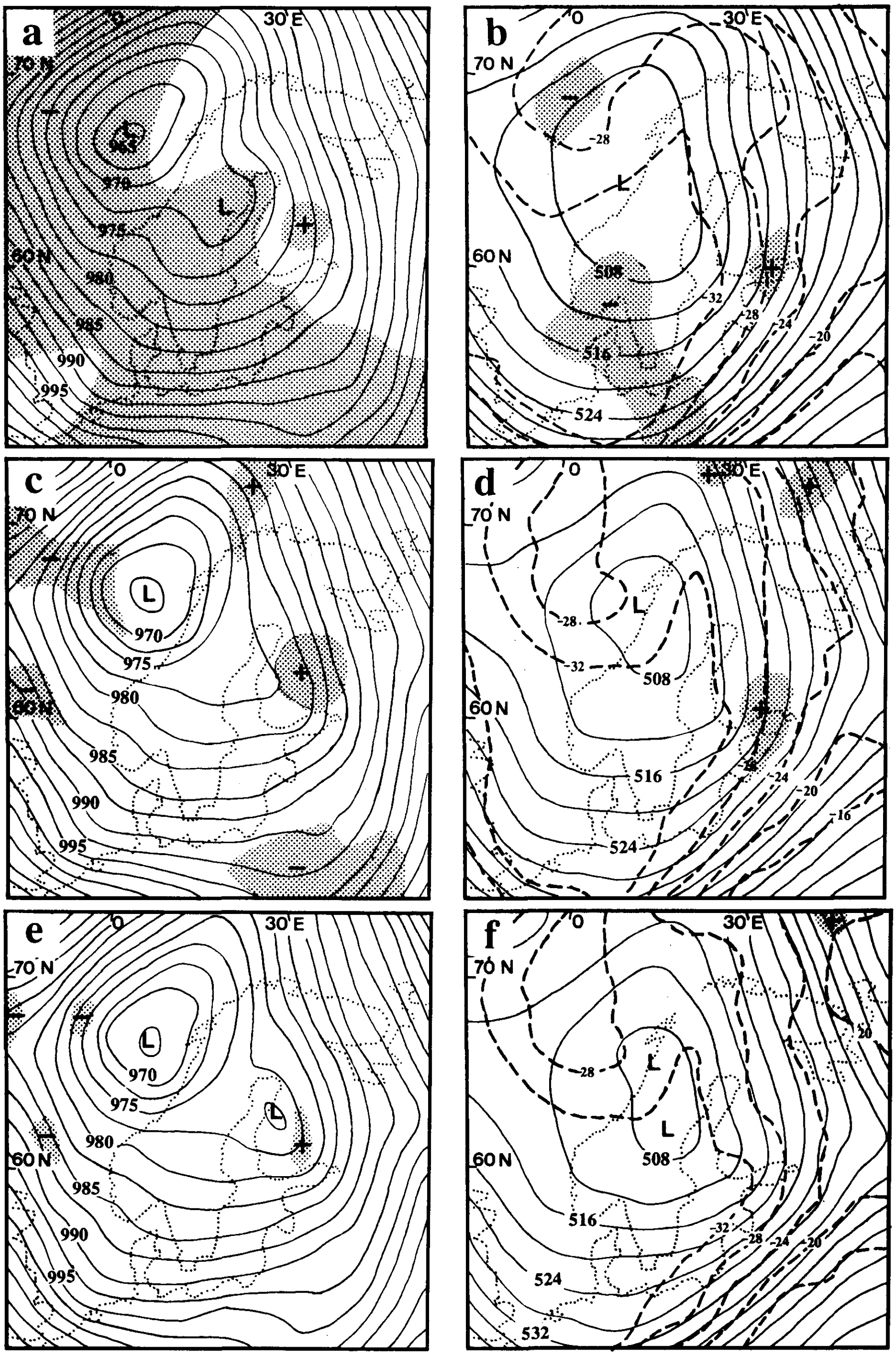


*Fig. 9.* Surface (left) and 500 mb (right) HIRLAM forecasts valid at 12 GMT, 23 October 1986 (a, b +24 h; c, d +12 h; e, f +6 h forecasts). For the surface forecasts, pressure (solid lines) is given; for the 500 mb level geopotential height (solid) and temperature (dashed) are given. Stippling denotes absolute values of forecast error (forecast-analysis): more than 2.5 mb for the surface pressure; more than 40 m for 500 mb geopotential height. The sign of the error is indicated in the figure (+ or −).

the HIRLAM Cray version of the Swedish–Danish limited area model (Unden, 1982; see also Gustafsson et al., 1986), which has its origins in the ECMWF grid point model.

The horizontal resolution of the model is 0.5° × 0.5° (55 km × 55 km) in rotated latitude–longitude coordinates. In the vertical, 12 $\sigma$ levels were used. A semi-implicit time scheme with a 4 min time step was used in the time integration. The model physics is mainly based on the ECMWF grid point model physics package. For season-dependent (climatic) fields, such as that of the sea-surface temperature, the monthly climatological mean was used, which was close to the observed sea surface temperature. For further details, see reports mentioned above in this section.

We next discuss the simulations made with the HIRLAM system. Data assimilation (with a 6 h cycle) was run for a 3-day period (from 12 GMT 20 October to 12 GMT 23 October). Forecasts of 24 h, 12 h and 6 h, all valid at 12 GMT 23 October (when the low was most intense) were run. Forecasts longer than 24 h did not give any clear signs of the meso-scale cyclogenesis.

In the 24-h 500 mb forecast (Fig. 9b), the trough over southern Finland is too smooth (maximum forecast error 60 m) and the 500 mb meso-scale temperature wave present in the analysis over southern Finland (Fig. 8) is not reproduced in the forecast (Fig. 9b). In the 12-h forecast (Fig. 9d) valid at 12 GMT 23 October, the trough over the Baltic Sea and southern Finland had not sharpened. In the 6-h forecast (Fig. 9f), the temperature wave has now appeared over central Finland, and there has been some deepening of the trough over southern Finland (maximum forecast error 30 m).

In the 24-h HIRLAM surface forecast (Fig. 9a), the surface trough and the pressure gradient are too weak in the area of the low, compared to the verifying analysis in Fig. 7. In the 12-h forecast (Fig. 9c), the overall pressure configuration is much better than the erroneous pattern in the 24-h forecast, but the surface pressure gradient has not strengthened significantly and the local maximum forecast error has increased from 3 mb to 6 mb. In the 6-h forecast (Fig. 9e), there is a small closed surface low, but its location is incorrect. Thus it can be said that the surface forecasts produced by the HIRLAM model are all in disagreement with the verifying surface pressure patterns over southern Finland to a greater or lesser extent, depending on the forecast length.

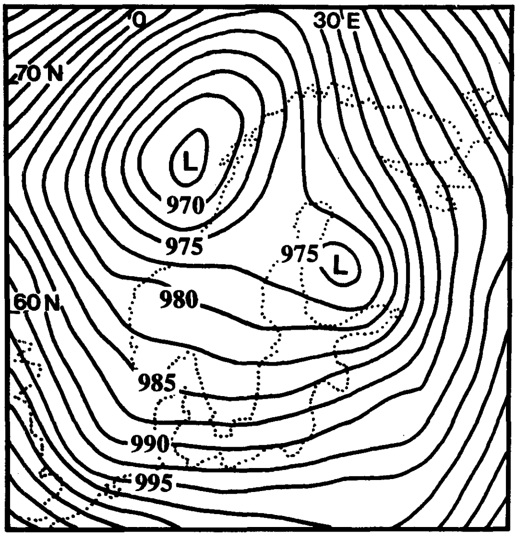


*Fig. 10.* HIRLAM surface analysis valid at 12 GMT, 23 October 1986. Notation as in Fig. 9.

Even the HIRLAM surface analysis (Fig. 10) failed to describe the meso-scale low over southern Finland in detail. The error in the HIRLAM surface pressure analysis is only about 2 mb, but the shape of the meso-scale part of the pressure pattern differs greatly from the subjective analysis (Fig. 7). Also, the analysed surface wind speeds over the Gulf of Finland are only about 10 m s$^{-1}$, while a wind speed of 26 m s$^{-1}$ was observed. Because of the high resolution of the HIRLAM model, it is natural that the HIRLAM forecasts and analyses were more accurate than those of ECMWF (not shown), which gave maximum surface winds of 8 m s$^{-1}$ over the Gulf of Finland.

## 4. Discussion and conclusions

In our case, synoptic and meso-scale flow patterns were not in accordance with either so-called "polar low" or with "comma cloud" concepts. In the early stages of development, the cyclone studied mainly exhibited polar-low properties, since the convective meso-scale low was situated well within the cold air mass. Later on, properties of comma clouds, i.e., the baroclinic synoptic-scale flow with a comma-shaped cloud pattern, became dominant. Thus, the case studied supports the view that some polar air vortices are difficult to categorize as either polar lows or comma clouds (see, e.g., Businger, 1987).

Two kinds of initial forcing mechanism in the intense cyclone development over the Baltic Sea at about 00 GMT 23 October 1986 may be envisaged. Firstly, upper-level positive vorticity advection generated upward motion. According to the HIRLAM analysis (not shown), the vertical motion was strongest at the 500 mb level. The importance of this upper forcing can be deduced from the fact that of the two successive meso-scale cloud patterns A and B, only the latter had large values of positive vorticity advection at 500 mb (see Fig. 4). Secondly, heat fluxes from a sea of small areal extent (width about 500 km), surrounded by cooler land areas, generated positive vertical motion.

The vertical motion triggered organized and enhanced cumulonimbus convection over the northern Baltic Sea. The intensification of the low was aided by the release of latent heat. At 00 GMT, the temperature and geopotential fields were in phase at all pressure levels and there was no temperature advection in the sounding approximately 100 km south of the developing cyclone. In this sounding, only weak vertical shear (7 m $s^{-1}$ between 850 mb and 500 mb) can be seen. We conclude that the initial formation of the low was most likely forced by organized cumulonimbus convection (CISK) and not by baroclinic instability.

During the later stages, baroclinic instability eventually took over responsibility for the development of the low. A short (1000 km) temperature wave can clearly be seen ahead of the surface cyclone in the 500 mb analysis (Fig. 8). Short-wave baroclinic instability became possible when the sensible heat flux from the sea reduced the overall static stability of the lowest troposphere (see e.g., Staley and Gall, 1977). Although the relative role of CISK and baroclinic instability during different stages of development has not been quantitatively tested by using numerical models, the data observed supports the point of view presented.

Many case studies of polar lows have shown that they are primarily baroclinic disturbances, which have been aided by diabatic effects (Reed, 1979; Sardie and Warner, 1985 and Orlanski, 1986). In the case studied here, the mechanisms seem to have acted in the reverse order. The initial mechanism was organized convection. Later on, baroclinic instability took over the dominant role. This is in accordance with the proposal of Forbes and Lottes (1985). It has been concluded in some recent studies that depending on the amount of heating and its vertical distribution, either convective or baroclinic processes may dominate the development of polar air vortices. Some systems appear to lie in the transition region between these two mechanisms (see Craig and Cho, 1988).

The failure of the HIRLAM forecasts and analyses in describing the meso-scale surface pressure pattern was probably due to too coarse a resolution (horizontally 55 km × 55 km) and to problems in parameterization of deep convection and heat fluxes from the sea (see e.g., Anthes et al., 1983; Kuo and Reed, 1988). The case studied has been selected in the Finnish Meteorological Institute for further simulations to test the role of different forcing mechanisms by using the present version of the HIRLAM model.

## 5. Acknowledgements

We would like to thank Dr. Juhani Rinne for initiating and supporting the use of this case as one of the tests for the HIRLAM model. We extend our appreciation to Dr. Hannu Savijärvi for discussing the manuscript and to Ms. Elena Saltikoff for drawing the figures.

## REFERENCES

Anthes, R. A., Kuo, Y-H. and Gyakum, J. R. 1983. Numerical simulations of a case on explosive marine cyclogenesis. *Mon. Wea. Rev. 111*, 1174–1188.

Bijlsma, S. J. and Hafkenscheid, L. M. 1984. A non-linear normal mode initialization method for a limited area model. Internal KNMI Note, 38 pp.

Bratseth, A. M. 1985. A note on CISK in polar air masses. *Tellus 37A*, 403–406. Polar low special issue.

Browning, K. A. and Hill, F. F. 1985. Mesoscale analysis of a polar trough interacting with a polar front. *Quart. J. Roy. Meteor. Soc. 111*, 445–462.

Businger, S. 1985. The synoptic climatology of polar low outbreaks. *Tellus 37A*, 419–432.

Businger, S. 1987. The synoptic climatology of polar air outbreaks over the Gulf of Alaska and the Bering Sea. *Tellus 39A*, 307–325.

Craig, G. and Cho, H-R. 1988. Cumulus heating and CISK in the extratropical atmosphere. Part I: Polar lows and comma clouds. *J. Atmos. Sci. 43*, 2622–2640.

Forbes, G. S. and Lottes, W. D. 1985. Classification of meso-scale vortices in polar air streams and the influence of the large scale environment on their evolutions. *Tellus 37A*, 132–155.

Gustafsson, N., Järvenoja, S., Kållberg, P. and Woetmann Nielsen, N. 1986. Basline experiments with a high resolution limited area model. *HIRLAM Technical Report No. 1*, Copenhagen, 17 November 1986. 87 pp.

Gustafsson, N. and Järvenoja, S. 1987. Sensitivity tests with a limited area version of the ECMWF analysis scheme. *HIRLAM Technical Note No. 3*, Copenhagen, October 1987. 26 pp.

Harrold, T. W. and Browning, K. A. 1969. The polar low as a baroclinic disturbance. *Quart. J. Roy. Meteor. Soc. 95*, 710–723.

Kuo, Y-H. and Reed, R. J. 1988. Numerical simulation of an explosively deepening cyclone in the Eastern Pacific. *Mon. Wea. Rev. 116*, 2081–2105.

Locatelli, J. D., Hobbs, P. V. and Werth, J. A. 1982. Mesoscale structures of vortices in polar air streams. *Mon. Wea. Rev. 110*, 1417–1433.

Lystad, M. (ed.) 1986. *Polar lows in the Norwegian, Greenland and Barents Sea.* Polar Lows Project, Final Report. The Norwegian Meteorological Institute, Oslo, Norway.

Lönnberg, P. and Shaw, D. 1987. ECMWF data assimilation scientific documentation, Research Manual 1.

Mansfield, D. A. 1974. Polar lows: the development of baroclinic disturbances in cold air outbreaks. *Quart. J. Roy. Meteor. Soc. 100*, 541–554.

Økland, H. 1987. Heating by organized convection as a source of polar low intensification. *Tellus 39A*, 397–407.

Økland, H. and Schyberg, H. 1987. On the contrasting influence of organized moist convection and surface heat flux on a barotropic vortex. *Tellus 39A*, 385–389.

Orlanski, I. 1986. Localized baroclinicity. A source for meso-alpha cyclones. *J. Atmos. Sci. 43*, 2857–2885.

Rasmussen, E. 1977. The polar low as a CISK-phenomenon. *Report No. 6*, University of Copenhagen, Institution for theoretical meteorology.

Rasmussen, E. 1979. The polar low as an extratropical CISK-disturbance. *Quart. J. Roy. Meteor. Soc. 105*, 531–549.

Rasmussen, E. 1981. An investigation of polar low with a spiral cloud structure. *J. Atmos. Sci. 38*, 1785–1792.

Rasmussen, E. 1985. A case study of a polar low development over the Barents Sea. *Tellus 37A*, 407–418.

Reed, R. J. 1979. Cyclogenesis in polar air streams. *Mon. Wea. Rev. 107*, 38–52.

Reed, R. J. and Blier, W. 1986. A case study of comma cloud development in the Eastern Pacific. *Mon. Wea. Rev. 114*, 1681–1695.

Sardie, J. M. and Warner, T. T. 1983. On the mechanism for the development of polar lows. *J. Atmos. Sci. 40*, 869–881.

Sardie, J. M. and Warner, T. T. 1985. A numerical study of the development mechanisms of polar lows. *Tellus 37A*, 460–477.

Staley, D. O. and Gall, R. L. 1977. On the wavelength of maximum baroclinic instability. *J. Atmos. Sci. 34*, 1679–1688.

Uccellini, L. W. 1986. The possible influence of upstream upper-level baroclinic processes on the development of the QE II storm. *Mon. Wea. Rev. 114*, 1019–1027.

Unden, P. 1982. The Swedish limited area model. SMHI Reports. Meteorology and Climatology, *RMK 35*, 33 pp.

Zick, C. 1983. Methods and results of an analysis of comma cloud developments by mean of vorticity fields from upper tropospheric satellite wind data. *Meteorol. Rdsch. 36*, 69–84.